

# Subtropical climate conditions and mangrove growth in Arctic Siberia during the early Eocene

Guillaume Suan<sup>1\*</sup>, Speranta-Maria Popescu<sup>2</sup>, Jean-Pierre Suc<sup>3</sup>, Johann Schnyder<sup>3</sup>, Séverine Fauquette<sup>4</sup>, François Baudin<sup>5</sup>, Daichi Yoon<sup>3</sup>, Karsten Piepjohn<sup>5</sup>, Nikolay N. Sobolev<sup>6</sup>, and Loïc Labrousse<sup>3</sup>

<sup>1</sup>Université Claude Bernard Lyon 1, ENS-Lyon, CNRS, UMR 5276 LGL-TPE, F-69622 Villeurbanne, France

<sup>2</sup>GeoBioStratData.Consulting, 385 route du Mas Rillier, 69140 Rillieux la Pape, France

<sup>3</sup>Sorbonne Universités, UPMC Université Paris 06, CNRS, Institut des Sciences de la Terre Paris (ISTeP), 75005 Paris, France

<sup>4</sup>Institut des Sciences de l'Évolution, Université de Montpellier, CNRS 5554, IRD, Place Eugène Bataillon, 34095 Montpellier cedex 5, France

<sup>5</sup>Bundesanstalt für Geowissenschaften und Rohstoffe, Geozentrum Hannover, Stilleweg 2, 30655 Hannover, Germany

<sup>6</sup>A.P. Karpinsky Russian Geological Research Institute (VSEGEI), 74, Sredny prospect, 199106, St. Petersburg, Russia

## ABSTRACT

The early Eocene (ca. 56–47.8 Ma) was an interval of exceptional warmth with reduced pole-to-equator temperature gradients. Climate proxies indicate mean annual air temperatures (MATs) and sea-surface temperatures (SSTs) exceeding 8–18 °C and frost-free, mild winters in polar areas, features that have proven difficult to reproduce with the most elaborate climate models. A full appraisal of the early Eocene polar climate has been, however, limited by possible seasonal biases associated with geochemical proxies and the lack of data from the vast Eurasian Arctic. Here we present multiproxy data from lower-middle Eocene coastal plain sediments of the New Siberian Islands (Russia) showing that taxodioid Cupressaceae, palms, and the mangrove *Avicennia* grew in Arctic Siberia above 72°N under air temperatures averaging 16–21 °C annually and 5.5–14 °C in winter. Kaolinite contents are exceptionally high (up to 60% of clay assemblages) and comparable to those found in present-day subtropical soils formed under high mean annual precipitation (MAP >1000 mm) and warm (MAT >15 °C) conditions. The *Avicennia* pollen records the northernmost mangrove growth ever documented and indicates early Eocene SSTs exceeding 13 °C in winter and 18 °C in summer. Considering the high MAP estimated for Arctic Siberia and other pan-Arctic landmasses, we propose that the heat from warm river waters draining into the Arctic might have amplified early Eocene polar warmth. Our results provide the first climate constraints for the early Eocene of Arctic Siberia and support the view that most climate models underestimate polar warming in greenhouse conditions.

## INTRODUCTION

Paleoclimate proxies indicate exceptional warmth in both the southern and northern high latitudes during the early Eocene, with mean annual sea-surface temperatures (SSTs) and mean annual air temperatures (MATs) exceeding 8 °C to 18 °C for some proxies (Eldrett et al., 2009; Huber and Caballero, 2011; Pross et al., 2012; Weijers et al., 2007; West et al., 2015). Available data for the Eocene of the Arctic may, however, not fully capture early Eocene polar conditions, as the data are primarily derived from the North American margin and lacking for large areas bordering northern Eurasia (Huber and Caballero, 2011; Fig. 1). Besides, the high SST and MAT based on tetraether lipids from Integrated Ocean Drilling Program (IODP) Site 302 in the central Arctic (Fig. 1) may potentially include a warm bias due to seasonal production or allochthonous input (Ho et al., 2014; Sluijs et al., 2009; Weijers et al., 2007), while pollen

records from offshore marine cores may suffer from biases linked to long-distance oceanic transport (Eldrett et al., 2009; Pross et al., 2012). It is therefore crucial to extend the spatial coverage of early Eocene polar and subpolar temperature data with multiproxy evidence to more robustly constrain high-latitude climate during this key interval.

To gain further understanding of early Eocene climate in Arctic Siberia, we performed palynological, geochemical, and mineralogical analyses (see the GSA Data Repository<sup>1</sup>) of coastal plain sediments recovered during the CASE (Circum Arctic Structural Events) 13 expedition on the Belkovsky and Faddeevsky Islands (New Siberian Islands [NSI], Russia). The position of the NSI with regard to Eurasia has undergone little change since Eocene times

<sup>1</sup>GSA Data Repository item 2017168, maps, biostratigraphy and descriptions of sample localities, methods, and full data, is available online at <http://www.geosociety.org/datarepository/2017/> or on request from [editing@geosociety.org](mailto:editing@geosociety.org).

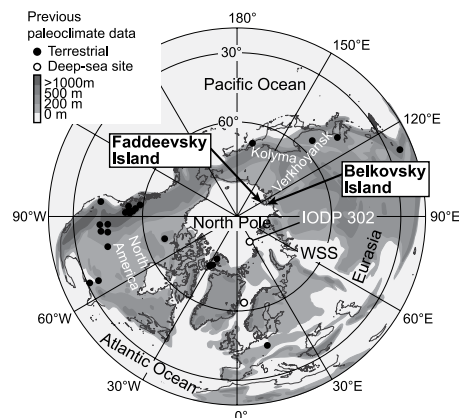
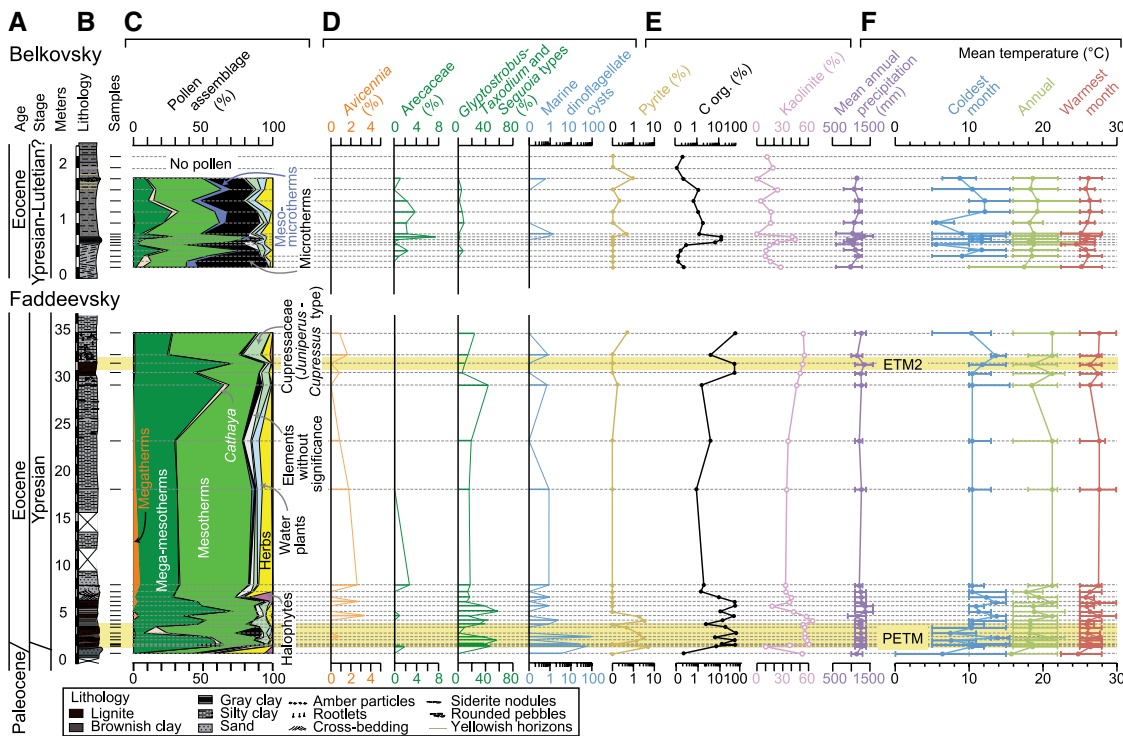


Figure 1. Location of studied sites with respect to early Eocene paleogeography (Markwick, 2007) of Northern Hemisphere, showing location of previous early Eocene temperature estimates from terrestrial (black dots) and deep-sea sites (gray dots) (Huber and Caballero, 2011; West et al., 2015; Wolfe et al., 2012). WSS—West Siberian Sea; IODP 302—Integrated Ocean Drilling Program Site 302.

(Fig. 1), with an estimated paleolatitude >72°N (Shephard et al., 2013; see the Data Repository). The age of the NSI successions was established using a combination of palynological and carbon isotope data (Figs. DR2–DR5 and text in the Data Repository). Accordingly, the Faddeevsky Island succession was deposited between the Paleocene-Eocene Thermal Maximum (PETM) and Eocene Thermal Maximum 2 (ETM2) of the early Eocene, 56–54 Ma, when temperature rose globally before reaching a long-term maximum known as the Early Eocene Climate Optimum (EECO; Zachos et al., 2008); sediments at Belkovsky Island were deposited near the early to middle Eocene transition ca. 48 Ma, when global temperatures declined at the termination of the EECO (Zachos et al., 2008). The recorded NSI pollen taxa were grouped in pollen diagrams (Fig. 2) according to classification of living

\*E-mail: [guillaume.suan@univ-lyon1.fr](mailto:guillaume.suan@univ-lyon1.fr)



**Figure 2.** Palynology, mineralogy, and geochemistry of New Siberian Islands Eocene coastal sediments. **A:** Age. **B:** Lithology (see Fig. DR2 [see footnote 1] for details) and sampled horizons. **C:** Synthetic pollen diagram. **D:** Abundance of selected palynomorphs. Pollen contents are expressed relative to total pollen sum; marine dinoflagellate cysts are expressed with respect to 100 pollen grains. **E:** Pyrite, organic carbon (C org.), and kaolinite contents. **F:** Precipitation and temperatures deduced from climatic amplitude method (Fauquette et al., 1998). Error bars represent minimum and maximum values returned by the method. PETM—Paleocene-Eocene Thermal Maximum; ETM2—Eocene Thermal Maximum 2.

plants (Nix, 1982) with respect to MAT. Terrestrial MAT, mean annual precipitation (MAP), and mean temperatures of the coldest (MTC) and warmest (MTW) months were reconstructed using the “Climatic Amplitude Method” on low-altitude pollen assemblages (Fauquette et al., 1998; see the Data Repository).

## RESULTS

The lower Eocene strata from Faddeevsky Island, representing coastal plain environments with both fluvial and marine influence, reveal a highly diverse pollen flora comprising 117 taxa (Table DR1 in the Data Repository). The preeminent characteristic of this flora is the occurrence of *Avicennia* (Fig. 3). The pollen assemblages are dominated by trees, particularly mega-mesotherms, namely prevalent *Glyptostrobus-Taxodium* and *Sequoia* types, *Engelhardia*, *Nyssa*, and palms (Arecaceae), along with mesotherms such as *Carya*, *Zelkova*, and *Castanea-Castanopsis*. Meso-microtherms and microtherms are represented by subordinate amounts of conifer pollen grains (Fig. 2). Several levels have yielded substantial amounts of dinoflagellate cysts (Fig. 2), which in the basal part reach up to 90 cysts for 100 pollen grains and mostly belong to *Apectodinium*, a thermophilic taxon that spread globally during PETM warming (Sluijs et al., 2009; Weijers et al., 2007).

The pollen flora from Belkovsky Island, ~5 m.y. younger and preserved in fluvial channel, floodplain, and swamp sediments, is composed of 76 taxa and also dominated by trees, but includes fewer mega-mesotherms such as prevalent *Glyptostrobus-Taxodium* and *Sequoia* types, *Engelhardia*, and palms (Arecaceae) (Table

DR2). Mesotherms constitute the dominant class of this pollen flora, with prevalent *Carpinus*, *Myrica*, *Pterocarya*, and *Quercus*. Pollen grains of conifers such as *Cathaya* (living today between 900 and 1900 m elevation in subtropical southwestern China), *Tsuga* (meso-microtherm), and *Abies* and *Picea* (microtherms) are also abundant. Water plants are abundant throughout the section, while salt marsh plants have not been recorded. Dinoflagellate cysts have been recorded in low abundances in only three samples (Fig. 2).

The obtained MAT, MTC, MTW, and MAP estimates are given for each pollen spectrum as an interval and a weighted mean (i.e., “most likely value”; see the Data Repository). In the Faddeevsky Island record, the most likely values vary between ~16 and 21 °C for MAT, between ~6 and 14 °C for MTC, between ~25 and 28 °C for MTW, and between 1100 and 1370 mm for MAP (Fig. 2). Slightly cooler and drier climate conditions were obtained for the ~5-m.y.-younger Belkovsky Island record, where most likely MAT values oscillate between 17 and 19 °C, MTC between 5.5 and 12 °C, MTW between 25 and 26 °C, and MAP between 980 and 1340 mm (Fig. 2).

The low maximum temperature ( $T_{max}$ ) values (Fig. DR3) and the thin post-Eocene sedimentary cover in the study area (Kos’ko and Trufanov, 2002) point to very limited burial and thermal overprinting, thus allowing reliable paleoclimatic interpretation of clay assemblages. Higher kaolinite proportions (>40%) in the Faddeevsky Island than in the Belkovsky Island sediments (<20%–40%) suggest warmer and more humid, highly hydrolyzing conditions. Higher kaolinite

contents occur in levels dominated by megamesotherms; conversely, higher chlorite and illite contents, indicative of source rocks of the nearby Verkhoyansk Range (Popp et al., 2007) and reflecting high detrital inputs and dynamic erosion of the hinterland (Chamley, 1989), occur in levels with higher abundance of meso-microtherms and microtherms (Fig. 2; Fig. DR3).

## DISCUSSION

### Source of the Pollen Grains

Several features indicate that long-distance transport of allochthonous pollen grains from lower latitudes cannot explain the dominance of mega-mesotherms to mesotherms in the NSI. First, pollen grains from lower latitudes would have accumulated preferentially in higher-energy

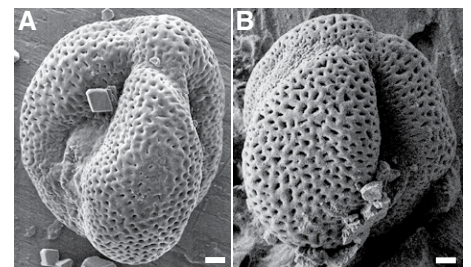


**Figure 3.** Early Eocene and modern pollen grains of *Avicennia*. **A:** Faddeevsky Island, Russia (sample GS127, 6.5 m [Fig. 2]). **B:** *Avicennia officinalis* L. (Lyon Herbarium [at Université Claude Bernard Lyon 1, Lyon, France] no. 18272). Scale bars are 2  $\mu$ m. These tricolpate or tricolporate equiaxial to slightly longiaxial pollen grains are characterized by long and largely opened colpi and homobrochate reticulum with dense muri.

fluvial channel deposits and comparatively less in more-restricted, clay-rich swamp deposits; the opposite relationship is recorded at both sites, where mega-mesothermal *Glyptostrobus-Taxodium* and *Nyssa* dominate in lignite beds rich in organic carbon (up to 60%; Fig. 2), amorphous organic matter, amber, and clay minerals (Fig. DR3), all indicative of water-logged, poorly oxygenated swamps or wetlands. Conversely fluvial, cross-bedded sands record lower amounts of mega-mesotherms and higher amounts of bisaccate conifer pollen advantaged in fluvial transport (*Cathaya*, *Pinus*, *Cedrus*, *Tsuga*, *Abies*, *Picea*; Fig. 2). These sands also show higher proportions of chlorite and illite, likely sourced from the Verkhoysk Range (Popp et al., 2007; Fig. 1; Fig. DR3). A similar association of mangroves and evergreen broad-leaved forests growing near deciduous temperate-cool forest occurs today in southeastern China and Taiwan, where forests with *Picea*, *Tsuga*, and *Abies* develop in high-altitude (>2300 m) hinterland characterized by much cooler MATs and common snow and frost events (see the Data Repository). These features imply that the transport of allochthonous pollen grains introduced a “cold” bias rather than a “warm” bias in the NSI palynofloras.

Secondly, *Avicennia*, due to its low pollen productivity, today occurs only in low abundances at very short distances from its source (Somboon, 1990). On Faddeevsky Island, the proximity of marine to brackish waters suggested by *Avicennia* and other halophytes (Table DR1) is supported by the high pyrite contents recorded in beds enriched in dinoflagellate cysts (Fig. 2), which we interpret as resulting from enhanced marine sulfate availability by brief tidal or eustatic flooding. Similarly, *Avicennia* increases in abundance with *Areaceae* and *Poaceae* (Fig. 2), a relation also recorded in some modern mangrove sediments (Somboon, 1990) that we interpret as reflecting temporal changes in the proximity of source areas in mangrove-dominated tidal creeks and estuaries. All of these features imply on-site growth of *Avicennia* at a paleolatitude >72°N, meaning that the NSI sediments record the highest-latitude mangrove known (as compared to previous findings of Eocene mangrove palms at paleolatitudes of 45°N and 65°S; Pole and Macphail, 1996).

### Marine Connectivity and Climate Conditions in Arctic Siberia

Modern *Avicennia* species reproduce by shedding propagules, which, contrarily to their pollen grains, disperse over relatively long distances through oceanic currents, and may strand and settle when favorable conditions are met (Quisthoudt et al., 2012). Assuming that Eocene *Avicennia* had a similar ecology and was not a native taxon of the Arctic, its appearance in the NSI during the earliest Eocene warming thus supports the idea that the coeval flooding

connected the Arctic Ocean with more southern basins (Frieling et al., 2014), possibly through the West Siberian Sea (Fig. 1). In addition, modern *Avicennia* species are generally limited to warm coastlines characterized by annual SST ( $SST_A$ ) of 22.6 °C and SST of the coldest month ( $SST_C$ ) of 18.8 °C (Quisthoudt et al., 2012) and cannot tolerate events of extremely cold air temperatures (<−4 °C; Cavanaugh et al., 2014). However, thanks to warm currents, *Avicennia* is the only mangrove that is not restricted to the tropics; at its coldest limit in New Zealand and eastern Australia, it occurs at  $SST_C$  of 12.7 °C,  $SST_A$  of 15.6 °C, and warmest month SST of 18.8 °C (Quisthoudt et al., 2012). We take these upper latitudinal values as minimum SST estimates for Arctic Siberia (Fig. 4), as the NSI mangrove lacks *Rhizophora* that even at its coldest limits has slightly higher SST requirements ( $SST_C > 16.4$  °C,  $SST_A > 20.8$  °C; Quisthoudt et al., 2012). Our SST estimates are close to those of ~13 °C estimated for Pacific, Atlantic, and Southern Ocean deep waters during the early Eocene, which likely record  $SST_C$  of marginal regions near Antarctica (Hollis et al., 2012; Lear et al., 2000). Our results thus imply that both poles experienced comparable SSTs during the early Eocene (Fig. 4).

Independent support for the high MAT and MAP estimated from the low-altitude pollen assemblages comes from the unusually high kaolinite contents in lignite beds (>40%; Fig. 2), which are nowadays found mostly in soils at tropical to subtropical latitudes (Griffin et al., 1968) characterized by elevated warmth (MAT >15 °C) and humidity (MAP >1000 mm; Robert and Kennett, 1994). In accordance with the higher pollen-derived MAT and MAP, the higher kaolinite contents of Faddeevsky Island point to moister and warmer conditions during the earliest Eocene (Fig. 2).

### Implications for Climate Models

Our multiproxy NSI data are in line with the high MAT (~18–25 °C; Weijers et al., 2007) and SST (~18–25 °C; Sluijs et al., 2009) values based on tetraether membrane lipids recovered from lower Eocene strata of IODP Site 302, and with the high MAT (8 and 17 °C) and MTC (3–9 °C) values indicated by floral and faunal data from lower to middle Eocene strata of Arctic Canada and Greenland (Eldrett et al., 2009; Huber and Caballero, 2011; West et al., 2015; Wolfe et al., 2012; Fig. 4). Our nearshore MAT values are, however, slightly higher than previous paleobotanical estimates (Fig. 4), possibly because they do not include a cool paleoelevation bias (Huber and Caballero, 2011).

In any case, the subtropical SST, MTC, and MAT values recorded in Arctic Siberia demonstrate that the early Eocene extreme warmth was a pan-Arctic phenomenon and reinforce the view that most models unrealistically

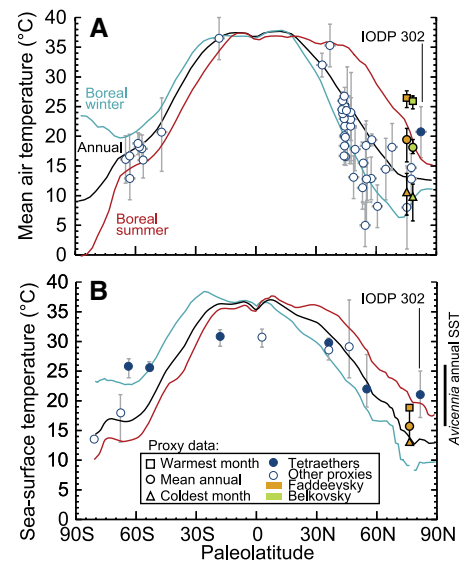


**Figure 4. Comparison of Eocene latitudinal temperature gradients from proxies and models. A: Mean terrestrial air temperatures. B: Mean terrestrial air temperatures (A) and sea-surface temperatures (B) estimated using paleobotanical, oxygen isotope, and clumped isotope proxies (white dots) and tetraether lipids (blue dots; data from Weijers et al., 2007; Sluijs et al., 2009; Huber and Caballero, 2011; Frieling et al., 2014; Hollis et al., 2012). Paleolatitude of younger Belkovsky Island (Russia) record (early to middle Eocene) is the same as that of Faddeevsky Island (earliest Eocene) but has been shifted by 5° for illustration purposes. Black, red, and blue lines respectively show annual, warmest month, and coldest month zonal average temperatures obtained with Eocene climate models with 4480 ppmv CO<sub>2</sub> equivalent (Hollis et al., 2012; Huber and Caballero, 2011). IODP 302—Integrated Ocean Drilling Program Site 302.**

simulate greenhouse climates (e.g., Sagoo et al., 2013). State-of-the-art climate models can indeed only simulate such elevated temperatures using extremely high atmospheric CO<sub>2</sub> contents (>4000 ppm; Fig. 4), which are not only well above proxy estimates, but also difficult to explain in terms of CO<sub>2</sub> degassing (Huber and Caballero, 2011; Jagiecki et al., 2015; Hoareau et al., 2015). Suggested mechanisms to further warm polar areas include enhanced high-latitude wetland methane emissions, higher polar humidity, or highly modified configurations of cloud properties, water vapor, or atmospheric heat transport (Greenwood et al., 2010; Beerling et al., 2011; Kiehl and Shields, 2013; Sagoo et al., 2013). Increased humidity and wetland methane emissions are supported by our NSI data, but are sufficient alone (Kiehl and Shields, 2013; Sagoo et al., 2013) to explain the model-data discrepancies highlighted by our results.

An additional agent of polar warming that has attracted much less attention is the discharge of warm waters by Arctic rivers, a hydrological feedback linked to global temperatures and able to increase SST by several degrees in extant

pan-Arctic shelves (Whitefield et al., 2015, and references therein). In addition to the supply of considerable heat accumulated at lower latitudes, this discharge transports less dense, sediment-laden waters offshore, thereby decreasing the albedo of Arctic superficial waters and further warming polar areas (Whitefield et al., 2015). In this regard, our NSI clay mineral and pollen data show for the first time that the unusually high MAP (>1000 mm) previously evidenced for North American and Greenland margins (Eldrett et al., 2009; West et al., 2015; Wolfe et al., 2012; Greenwood et al., 2010) also characterized Arctic Siberia, and point to elevated rainfall in all pan-Arctic drainage basins. Such an increase in freshwater discharge is fully consistent with the anomalously low salinity reconstructed for the Eocene Arctic Ocean (Sluijs et al., 2009) and therefore deserves further testing as a powerful heat conveyor in future modeling efforts.

#### ACKNOWLEDGMENTS

The ship-based expedition CASE 13 to the New Siberian Islands was funded by the Bundesanstalt für Geowissenschaften und Rohstoffe (BGR), with logistical support of the A.P. Karpinsky Russian Geological Research Institute (VSEGEI). We thank the Université Paris 6 and Total S.A. for funding (Groupement Recherche et Industrie “Zones péri-Arctiques” to L.L.); Georges Barale (Université Lyon 1 Herbarium) for facilitating access to modern pollen grains; F. Fourel, M. Seris, F.S. Deaconu, O. Boudouma, and F. Savignac for technical assistance; Y. Donnadieu and J. Pross for helpful discussions; and J.S. Eldrett, A.B. Herman, and anonymous reviewers for constructive reviews.

#### REFERENCES CITED

- Beerling, D.J., Fox, A., Stevenson, D.S., and Valdes, P.J., 2011, Enhanced chemistry-climate feedbacks in past greenhouse worlds: Proceedings of the National Academy of Sciences of the United States of America, v. 108, p. 9770–9775, doi:10.1073/pnas.1102409108.
- Cavanaugh, K.C., Kellner, J.R., Forde, A.J., Gruner, D.S., Parker, J.D., Rodriguez, W., and Feller, I.C., 2014, Poleward expansion of mangroves is a threshold response to decreased frequency of extreme cold events: Proceedings of the National Academy of Sciences of the United States of America, v. 111, p. 723–727, doi:10.1073/pnas.1315800111.
- Chamley, H., 1989, *Clay Sedimentology*: Berlin Heidelberg, Springer, 623 p., doi:10.1007/978-3-642-85916-8.
- Eldrett, J.S., Greenwood, D.R., Harding, I.C., and Huber, M., 2009, Increased seasonality through the Eocene to Oligocene transition in northern high latitudes: *Nature*, v. 459, p. 969–973, doi:10.1038/nature08069.
- Fauquette, S., Guiot, J., and Suc, J.-P., 1998, A method for climatic reconstruction of the Mediterranean Pliocene using pollen data: *Palaeogeography, Palaeoclimatology, Palaeoecology*, v. 144, p. 183–201, doi:10.1016/S0031-0182(98)00083-2.
- Frieling, J., Iakovleva, A.I., Reichert, G.-J., Aleksandrova, G.N., Gnibidenko, Z.N., Schouten, S., and Sluijs, A., 2014, Paleocene–Eocene warming and biotic response in the epicontinental West Siberian Sea: *Geology*, v. 42, p. 767–770, doi:10.1130/G35724.1.
- Greenwood, D.R., Basinger, J.F., and Smith, R.Y., 2010, How wet was the Arctic Eocene rain forest? Estimates of precipitation from Paleogene Arctic macrofloras: *Geology*, v. 38, p. 15–18, doi:10.1130/G30218.1.
- Griffin, J.J., Windom, H., and Goldberg, E.D., 1968, The distribution of clay minerals in the World Ocean: *Deep Sea Research and Oceanographic Abstracts*, v. 15, p. 433–459, doi:10.1016/0011-7471(68)90051-X.
- Ho, S.L., et al., 2014, Appraisal of  $TEX_{86}$  and  $TEX_{86L}$  thermometries in subpolar and polar regions: *Geochimica et Cosmochimica Acta*, v. 131, p. 213–226, doi:10.1016/j.gca.2014.01.001.
- Hoareau, G., Bomou, B., van Hinsbergen, D.J.J., Carry, N., Marquer, D., Donnadieu, Y., Le Hir, G., Vrielynck, B., and Walter-Simonnet, A.V., 2015, Did high Neo-Tethys subduction rates contribute to early Cenozoic warming?: *Climate of the Past*, v. 11, p. 1751–1767, doi:10.5194/cp-11-1751-2015.
- Hollis, C.J., et al., 2012, Early Paleogene temperature history of the Southwest Pacific Ocean: Reconciling proxies and models: *Earth and Planetary Science Letters*, v. 349, p. 53–66, doi:10.1016/j.epsl.2012.06.024, erratum available at <http://dx.doi.org/10.1016/j.epsl.2013.06.012>.
- Huber, M., and Caballero, R., 2011, The early Eocene equable climate problem revisited: *Climate of the Past*, v. 7, p. 603–633, doi:10.5194/cp-7-603-2011.
- Jagniecki, E.A., Lowenstein, T.K., Jenkins, D.M., and Demicco, R.V., 2015, Eocene atmospheric  $CO_2$  from the nahcolite proxy: *Geology*, v. 43, p. 1075–1078, doi:10.1130/G36886.1.
- Kiehl, J.T., and Shields, C.A., 2013, Sensitivity of the Palaeocene-Eocene Thermal Maximum climate to cloud properties: *Philosophical Transactions of the Royal Society A: Mathematical, Physical and Engineering Sciences*, v. 371, 20130093, doi:10.1098/rsta.2013.0093.
- Kos'ko, M.K., and Trufanov, G.V., 2002, Middle Cretaceous to Eocene sequences on the New Siberian Islands: An approach to interpret offshore seismic: *Marine and Petroleum Geology*, v. 19, p. 901–919, doi:10.1016/S0264-8172(02)00057-0.
- Lear, C.H., Elderfield, H., and Wilson, P.A., 2000, Cenozoic deep-sea temperatures and global ice volumes from Mg/Ca in benthic foraminiferal calcite: *Science*, v. 287, p. 269–272, doi:10.1126/science.287.5451.269.
- Markwick, P.J., 2007, The palaeogeographic and palaeoclimatic significance of climate proxies for data-model comparisons, in Williams, M., et al., eds., *Deep-Time Perspectives on Climate Change: Marrying the Signal from Computer Models and Biological Proxies*: London, Geological Society of London, Micropalaeontological Society Special Publication, p. 251–312.
- Nix, H., 1982, Environmental determinants of biogeography and evolution in Terra Australis, in Barker, W.R., and Greenslade, P.J.M., eds., *Evolution of the Flora and Fauna of Arid Australia*: Frewville, Australia, Peacock Publishing, p. 47–66.
- Pole, M.S., and Macphail, M.K., 1996, Eocene Nypa from Regatta Point, Tasmania: Review of Palaeobotany and Palynology, v. 92, p. 55–67.
- Popp, S., Belolyubsky, I., Lehmkuhl, F., Prokopenko, A., Siegert, C., Spector, V., Stauch, G., and Diekmann, B., 2007, Sediment provenance of late Quaternary morainic, fluvial and loess-like deposits in the southwestern Verkhoyansk Mountains (eastern Siberia) and implications for regional palaeoenvironmental reconstructions: *Geological Journal*, v. 42, p. 477–497, doi:10.1002/gj.1088.
- Pross, J., et al., 2012, Persistent near-tropical warmth on the Antarctic continent during the early Eocene epoch: *Nature*, v. 488, p. 73–77, doi:10.1038/nature11300.
- Quisthoudt, K., Schmitz, N., Randin, C., Dahdouh-Guebas, F., Robert, E.R., and Koedam, N., 2012, Temperature variation among mangrove latitudinal range limits worldwide: *Trees* (Berlin), v. 26, p. 1919–1931, doi:10.1007/s00468-012-0760-1.
- Robert, C., and Kennett, J.P., 1994, Antarctic subtropical humid episode at the Paleocene-Eocene boundary: Clay-mineral evidence: *Geology*, v. 22, p. 211–214, doi:10.1130/0091-7613(1994)022<0211:ASHEAT>2.3.CO;2.
- Sagoo, N., Valdes, P., Flecker, R., and Gregoire, L.J., 2013, The Early Eocene equable climate problem: Can perturbations of climate model parameters identify possible solutions?: *Philosophical Transactions of the Royal Society A: Mathematical, Physical and Engineering Sciences*, v. 371, 20130123, doi:10.1098/rsta.2013.0123.
- Shephard, G.E., Müller, R.D., and Seton, M., 2013, The tectonic evolution of the Arctic since Pangea breakup: Integrating constraints from surface geology and geophysics with mantle structure: *Earth-Science Reviews*, v. 124, p. 148–183, doi:10.1016/j.earscirev.2013.05.012.
- Sluijs, A., Schouten, S., Donders, T.H., Schoon, P.L., Rohl, U., Reichert, G.-J., Sangiorgi, F., Kim, J.-H., Sinninghe Damsté, J.S., and Brinkhuis, H., 2009, Warm and wet conditions in the Arctic region during Eocene Thermal Maximum 2: *Nature Geoscience*, v. 2, p. 777–780, doi:10.1038/ngeo668.
- Somboon, J.R.P., 1990, Palynological study of mangrove and marine sediments of the Gulf of Thailand: *Journal of Southeast Asian Earth Sciences*, v. 4, p. 85–97, doi:10.1016/0743-9547(90)90008-2.
- Weijers, J.W.H., Schouten, S., Sluijs, A., Brinkhuis, H., and Sinninghe Damsté, J.S., 2007, Warm arctic continents during the Palaeocene-Eocene thermal maximum: *Earth and Planetary Science Letters*, v. 261, p. 230–238, doi:10.1016/j.epsl.2007.06.033.
- West, C.K., Greenwood, D.R., and Basinger, J.F., 2015, Was the Arctic Eocene ‘rainforest’ monsoonal? Estimates of seasonal precipitation from early Eocene megaflores from Ellesmere Island, Nunavut: *Earth and Planetary Science Letters*, v. 427, p. 18–30, doi:10.1016/j.epsl.2015.06.036.
- Whitefield, J., Winsor, P., McClelland, J., and Mendenhall, D., 2015, A new river discharge and river temperature climatology data set for the pan-Arctic region: *Ocean Modelling*, v. 88, p. 1–15, doi:10.1016/j.ocemod.2014.12.012.
- Wolfe, A.P., Csank, A.Z., Reyes, A.V., McKellar, R.C., Tappert, R., and Muehlenbachs, K., 2012, Pristine Early Eocene wood buried deeply in kimberlite from northern Canada: *PLoS One*, v. 7, e45537, doi:10.1371/journal.pone.0045537.
- Zachos, J.C., Dickens, G.R., and Zeebe, R.E., 2008, An early Cenozoic perspective on greenhouse warming and carbon-cycle dynamics: *Nature*, v. 451, p. 279–283, doi:10.1038/nature06588.

Manuscript received 30 August 2016  
 Revised manuscript received 8 February 2017  
 Manuscript accepted 11 February 2017

Printed in USA